



ELSEVIER

Available online at www.sciencedirect.com

ScienceDirect

journal homepage: www.elsevier.com/locate/he

Natural Gas/Hydrogen blends for heavy-duty spark ignition engines: Performance and emissions analysis

Luigi De Simio, Sabato Iannaccone, Chiara Guido^{*}, Pierpaolo Napolitano, Armando Maiello

National Research Council, Institute of Sciences and Technologies for Sustainable Energy and Mobility (CNR-STEMS), 80125 Napoli, Italy

HIGHLIGHTS

- Natural Gas/Hydrogen blends.
- Heavy-Duty spark ignition engines.
- Steady-state and transient engine operating modes.
- Performance, combustion and emission analysis.
- Particles number and size distribution characterization.

ARTICLE INFO

Article history:

Received 4 March 2023

Received in revised form

8 June 2023

Accepted 16 June 2023

Available online 12 July 2023

Keywords:

Natural Gas/Hydrogen blends

Heavy-Duty SI engine

Transient cycles

Combustion analysis

PN emissions

ABSTRACT

In view of the strong interest in the adoption of hydrogen as an alternative fuel for internal combustion engines, the authors present the results of an experimental activity aimed at evaluating the effect of hydrogen use on performance and emissions of a heavy-duty (HD) spark ignition engine.

The engine, installed on a test bench and working with compressed natural gas (CNG) in its standard version, has been fed with blends of CNG and H₂, at various percentages (15% and 25% of H₂ by volume) and tested in steady-state and transient driving conditions. The analysis in steady state was performed in two working modes: at the same combustion barycentre and at the same nitrogen oxides (NO_x) emissions of the pure CNG case, by means of proper spark advance calibrations.

A detailed combustion and emissions analysis were performed, highlighting a coherent response of the engine to the replacement of CNG with H₂. The NO_x increment tendency is easily counteracted by reduced SA settings, while total hydrocarbons and carbon oxides emissions reduction were measured when the blends were burnt. Consistent carbon dioxide emission mitigation was revealed, mainly in transient conditions, operated at the same ECU calibration of the pure CNG case.

The main novelty of the work is in providing an in-depth study of the engine behaviour to hydrogen addition in transient condition. The response of engine management system to different fuels when rapid speed and torque variations occur, were evaluated. In this sense, the study offers detailed information on the feasibility of the use of hydro methane

^{*} Corresponding author.

E-mail address: chiara.guido@stems.cnr.it (C. Guido).

<https://doi.org/10.1016/j.ijhydene.2023.06.194>

0360-3199/© 2023 The Authors. Published by Elsevier Ltd on behalf of Hydrogen Energy Publications LLC. This is an open access article under the CC BY license (<http://creativecommons.org/licenses/by/4.0/>).

in existing engine architecture; such mixtures can represent, in the next future, a probable fuel option in view of the oncoming decarbonization process.

Moreover, new insights on particle emission burning hydro-methane are presented. The results of engine-out PN emissions along a transient cycle revealed a correlation between particle emissions spikes with specific phases of the driving cycle and a trend in PN reduction in case of hydrogen addition.

© 2023 The Authors. Published by Elsevier Ltd on behalf of Hydrogen Energy Publications LLC. This is an open access article under the CC BY license (<http://creativecommons.org/licenses/by/4.0/>).

Definitions/Abbreviations

CNG	compressed natural gas
NO _x	nitrogen oxides
PN	particle number
ICE	internal combustion engine
EGR	exhaust gas recirculation
SA	spark advance
COVimep	coefficient of variation of indicated mean effective pressure
HD	heavy-duty
CO	carbon oxide
THC	total hydrocarbon
SI	spark ignition
LMG	liquefied methane gas
ECU	electronic control unit
ETC	European transient cycle
DI	direct injection
HR	heat release
ID	incubation duration
MFB ₁₀	mass fraction burned 10%
CD	combustion duration
MFB10-50	angle between MFB10 and MFB50
MFB ₅₀	mass fraction burned 50%
PSDF	particle size distribution function
WOT	wide open throttle
BMEP	brake mean effective pressure
CAD	crank angle degree
RORH	rate of heat release
HR%	heat release percentage
PFP	peak firing pressure
TDC	top dead center
LHV	lower heating value
EEV	environmental-friendly vehicles
BSFC	brake specific fuel consumption
EC	energy consumption
TWC	three-way catalyst

deposits depletion and market requests; the second is the need to satisfy the urgent environmental demands.

In this context, ICEs have seen a strong development leading to new technological solutions as internal or external exhaust gas recirculation (EGR) [1,2], variable valve timing [3], variable compression ratio [4], etc. Simultaneously, many researchers have focused on the use of alternative fuels for cleaner and more efficient combustion. An example is the dual fuel combustion concept, where the conventional diesel fuel and natural gas or a bio-derived fuel (like bio-gas) are used in diesel engines, reducing the amount of carbon atoms involved in the combustion process, thus lowering CO₂ emissions, while maintaining the target power request.

The spread of smart grids, that use renewable sources for production of electricity, is bringing out the need for efficient energy storage systems. In fact, renewable energies (solar or wind energy for example) are intermittent and variable and power plants are usually designed to manage less than the maximum possible power output, needing a way to supply sufficient power during absence of the renewable sources.

Hydrogen can be a good vector for energy storage since it can be synthesized from renewable resources. Hydrogen production techniques are consolidated and increasingly efficient [5,6]. In the last years, the studies on hydrogen as fuel for the transport sector have grown.

In [7,8], as example, the authors show the advantages in the usage of hydrogen as storage medium and transportation fuel, while [9] makes an analysis about its production cost and energy requirements at refuelling stations stating that minimal cost production is still an important requirement for hydrogen as an energy vector to be affirmed.

Studies on the use of hydrogen in ICEs report improvements of combustion efficiency along with reduced emissions, higher power density and better cost efficiency with respect to fuel cells [10–12]. Investigations, highlighting the distinctive combustion behaviour of hydrogen in internal combustion engines, are described in [13,14]. In the former, hydrogen combustion is analysed, showing that it is faster than gasoline combustion, with a strong dependence from engine speed at low air-fuel ratio and determining the spark advance (SA) modification for various operating conditions with respect to standard gasoline engine. In the latter, occurrence of abnormal combustion in a turbocharged engine and the effects of turbocharging on the combustion are considered, showing that the boost pressure increases the combustion speed maintaining noise at levels comparable to gasoline engines.

Introduction

In the last decades, internal combustion engines (ICE) have overcome many challenges to face two main issues. The first is the need to reduce fuel consumption, both for fossil fuel

In [15], the cyclic variation characteristics of a port fuel injection hydrogen engine is studied, determining the effect of fuel-air ratio, engine speed, ignition advance angle and hydrogen injection characteristics on the coefficient of variation of indicated mean effective pressure (COVimep). The results show that engine speed minimally affects the COVimep and no remarkable changes were observed with larger throttle positions. On the other hand, fuel-air ratio has a more remarkable effect on COVimep than the ignition advance angle.

In [16], Shivaprasad et al. analyse the spark timing dependence of gasoline-hydrogen blends up to 25% hydrogen by volume in a single-cylinder high-speed engine. The results show the presence of an optimization value for BMEP, brake thermal efficiency and specific energy consumption as a function of spark advance and these values are higher when using gasoline-hydrogen blends with 20% hydrogen by volume. Higher percentages of hydrogen cause losses in volumetric efficiency with reduced engine performance. Differences in combustion characteristics in terms of flame speed, quenching distance and ignition energy lead to a reduction of CO, HC and NO_x by increasing the ignition time for a given hydrogen mixing fraction and by increasing the hydrogen fraction for a given turn-on time.

Some studies are focused on the use of hydrogen in addition to compressed natural gas (CNG) in internal combustion engines. Efficiency, combustion and emission characterization for hydrogen/CNG blends have been studied in [17] testing a mixture at 29% by volume of hydrogen in an heavyduty (HD) engine and in [18] using a mixture with 55% by volume of hydrogen, while in [19] small amounts of hydrogen (below or equal to 8%) are considered. Differences can be outlined in the results considering low or high rotational speed and the different percentages of hydrogen. As general results, the cited works highlight the possibility of widening the lean burnability limits and of reducing carbon oxides and total hydrocarbons emissions in case of hydrogen addition to the fuel. Analysis about stability and emissions at idle are reported in [20] for hydrogen volume percentage from 0 to 50%. Hydrogen improves combustion tolerance to residual gas, bringing to enhanced stability of combustion at idle thus reducing fuel consumption. Besides, better combustion mitigates carbon oxides emissions and the presence of residual gas acts as a diluting agent reducing NO_x emissions. A numerical study using CONVERGE has been conducted by Fu et al. [21]. The authors' approach was to improve liquid methane gas (LMG) engine performance by means of hydrogen addition to LMG. Based on experimental data, a computational fluid dynamics model was built and employed to study the effect of different hydrogen energy fraction on combustion, thermodynamics and emissions of the LMG engine. Results show an increase of combustion speed bringing to higher cylinder peak pressure when hydrogen is substituted to LMG. Higher in cylinder temperature together with lean combustion condition used lead to a reduction of CO and CO₂ emissions but an increase of NO_x is reported which is caused by the increased in cylinder temperature.

An authors' previous paper [22] focussed on the use of natural gas/hydrogen mixture in a spark ignition engine, showing good results in terms of both combustion efficiency and emissions reduction, especially in case of lean burning

mixtures and high EGR percentages. Starting from these encouraging results, the aim of this work is to further investigate the advantages and drawbacks of hydrogen addition to CNG in an HD SI engine, deeply analysing the engine behaviour and emission not only in steady-state but also in transient conditions.

The blends characterization in steady-state operating conditions was performed following two approaches: at same combustion barycentre and at the same NO_x emissions of the pure CNG case. In this sense, the adoption of a programmable electronic control unit (ECU), led to calibrate the main engine control parameters, properly changing the SA values, when varying the percentage of hydrogen in the blends.

The analysis of the engine behaviour in transient conditions was performed running the engine along the European Transient Cycle (ETC) for heavy-duty emission certification and comparing the engine performances and emissions in case of pure CNG and of two mixtures at 15% and 25% by volume of hydrogen, adopting the same parameter calibration of the CNG case. Under transient conditions, it was also possible to evaluate the response of the management system of an existing engine to the fuel variation in case of the rapid speed and torque changes typical of the tested cycle. To this aim, the percentage of hydrogen in the mixtures was limited to 25% to avoid possible pre-ignition phenomena from hot spots that could occur increasing the hydrogen content [23]. In addition, the use of green H₂ in ICEs is seen as a way for the CO₂ reduction of existing vehicles, which would hardly be able to run in case of blends with high H₂ content, without strong modification in engine calibration and/or control architecture. Furthermore, the hydro methane blends, with hydrogen content lower than 30%, could be the most probable alternative fuel available in market in the next future, for safety and commercial feasibility reasons. In particular, the ECU response and the adaptability of the fuel injection system to different mixtures have been tested when the fuel formulation is modified from pure CNG up to 25% by volume of hydrogen. Indeed, the good running of the engine, mainly in transient conditions, depends on the possibility of maintaining precise control of the fuel-air mixture by means of the ECU, which, from the signal of the lambda probe corrects the injection time and the subsequent actuation of the gaseous injectors. The whole dynamics of operation is influenced by the change of fuel, requiring a different concentration with the air, to maintain the stoichiometric mixture and different fuel injection time values, compared to the original CNG case. Results highlight the possibility of easily using a mixture of 25% by volume of hydrogen in engines designed for natural gas, with good response both in terms of combustion efficiency and emissions. The present study was focused on the use of CNG/H₂ blends in a heavy-duty CNG engine equipped with a standard TWC. In this sense, stoichiometric mixture conditions were considered for the efficient working of the after-treatment systems. In future activity on pure hydrogen engine fuelling it will be interesting to investigate on lean operation that, as known, represents a potential tool in improving the engine efficiency with significant NO_x reduction [24,25].

A part of the activity, still ongoing, regarded the analysis of PN emissions with pure CNG and with CNG/hydrogen blends. The forthcoming stringent regulation on particles has

increased the interest in such emissions also in case of engines fed by gaseous fuels [26]. The aspect of particle number emissions from gas engines, in fact, is crucial. It is known that the main source of particles from this category of engines derives from the mechanisms of lube oil leakage in the combustion chamber [27,28].

Despite this, the available literature on particle formation and emission characterization from hydrogen engines is still limited. In case of premixed hydrogen combustion configuration, some literature studies report substantially lower particle formation for hydrogen enriched compressed natural gas mixture compared to other hydrocarbon fuels, so highlighting strong mitigation of carbon-based emissions [29,30].

Thawko et al. observed an opposite trend testing hydrogen in a direct injection (DI) gas engine [31]. In fact, even though a no-carbon fuel as hydrogen was used, it was observed an increase in PN formation in some operation conditions. At low engine load, combustion of pure hydrogen produces the lowest PN among the considered fuels but at high engine load pure methane determines lower PN than hydrogen. The combined effect of the flame quenching distance, fuel carbon content, and injection duration defines the PN formation in a DI ICE fed with a gaseous fuel, as stated from the authors.

The present paper enlarges the scientific literature, poor of data on this topic, providing some insights on PN emissions characterization along engine transient cycles. The results highlighted a strong correlation of particle emission spikes with specific phases of the cycle and a trend of emissions decreasing with hydrogen addition.

Experimental set-up and test program

Experimental tests were performed with pure CNG and two different CNG/hydrogen blends (15% and 25% hydrogen by volume). The engine used for the experimental tests is a HD SI turbocharged engine, compliant with Euro III regulation.

The main engine characteristics are shown in Table 1, while Fig. 1 shows the engine on the test bench. The engine has an experimental EGR system that, for the present activity, was bypassed by closing the recirculation valve. The engine is equipped with a dual volute turbine, with a waste gate acting only on one of the two inlets.

Table 1 – Main characteristics of the reference HD SI CNG engine.

Type	6-cylinder in line
Displacement	7800 cm ³
Bore x stroke	115x125 mm
Compression ratio	11:1
Rated power	200 kW @ 2100 rpm
Max torque	1100 Nm @ 1100–1650 rpm
Boost pressure	0.8 relative bar
Turbine	Dual volute with waste gate valve
Intercooler	Air to water (external line)
CNG feeding system	Electronic timed multi-point injection
Power density	25.6 kW/L

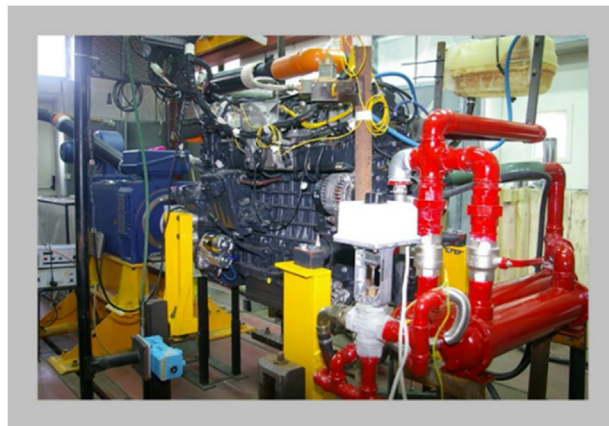


Fig. 1 – Engine installed on the test bench.

A programmable ECU enabled the access to the main control parameters (air to fuel ratio, SA, wastegate duty cycle, etc.) and allowed to change them during engine operation. Performances were tested on an asynchronous alternating current motor. Fuel flow rate was measured by means of a Coriolis mass flow meter. A piezoelectric pressure transducer from KISTLER (sensitivity 26 pC/bar) was installed in one of the six cylinders for in-cylinder pressure acquisition. Each pressure cycle was recorded as mean value of 100 consecutive cycles. Indicated signals were acquired through the AVL Indicom software. The apparent heat release (HR) curves were used to calculate the incubation duration (ID), or mass fraction burned 10% (MFB₁₀), as the period from the SA to 10% of HR, the combustion duration (CD) or mass fraction burned 10–50% (MFB₁₀₋₅₀), and MFB₅₀ (or combustion barycentre) as the angle at which 50% of heat is released.

Gaseous emissions were acquired through an exhaust gas analysis system; particulate emissions in terms of PN and particle size distribution function (PSDF) were measured using a differential mobility spectrometer DMS500 from Cambustion society. The differential mobility spectrometer classifies the total PN in nucleation mode (particles with diameter from about 5 nm to about 50 nm) and accumulation mode (particles with diameter from about 50 nm to about 1000 nm). The device measurements cover twenty dimensional classes of the particles. Table 2 reports the DMS500 sensitivity values according to the particle diameters. More details on measurement principle and characteristics/performances of the device can be found in [32].

A list of the main adopted instrumentations, with their measurement ranges and accuracies, is reported in Table 3. Temperature and pressure transducers were installed for a complete monitoring of the inlet and exhaust lines.

Table 2 – DMS500 sensitivity (RMS at 1 Hz).

Particle dimension	Sensitivity
10 nm	1.0*10 ³ (dN/dlogDp/cc)
30 nm	4.0*10 ²
100 nm	1.7*10 ²
300 nm	8.0*10 ¹

Table 3 – Instrumentation for emission and performance measurement.

Unit	Type	Range	Accuracy
Torque	Torque flange HBM T 10F	2000 Nm	±0.2% of range
Speed	Encoder heidenhain	3500 rpm	<±1 rpm
Power	AFA AVL dinamometer	280–315 kW @ 2000–3500 rpm	±0.2% of reading
Fuel	Micro motion elite	50 kg/h	<1% of reading
Air	ABB sensy flow P	1200 kg/h	±1% of reading
THC	MULTIFID 14 EGA	0–10000 ppm C3	0.5% of range
CH4		0–10000 ppm C1	
CO	URAS 14 EGA.	0–10%	<1% of range
NOX	CLD ecophysics	0–5000	<1% of range
CO2	URA 14 EGA	0–20%	1% of range
O2	MACROS 16 EGA	0–25%	0.5% of range

Table 4 – Characteristics of the tested fuels.

Fuel	α_{st}	LHV	ρ	H/C	C	H ₂	CO ₂
Unit	kg/kg	MJ/kg	kg/Sm ³	n/m	% mass	% mass	g/MJ
CNG	15.8	45.8	0.81	3.8	71.0	22.4	56.7
HCNG15	15.8	46.2	0.72	4.0	68.7	23.3	54.4
HCNG25	16.2	47.8	0.65	4.3	68.3	24.7	52.4

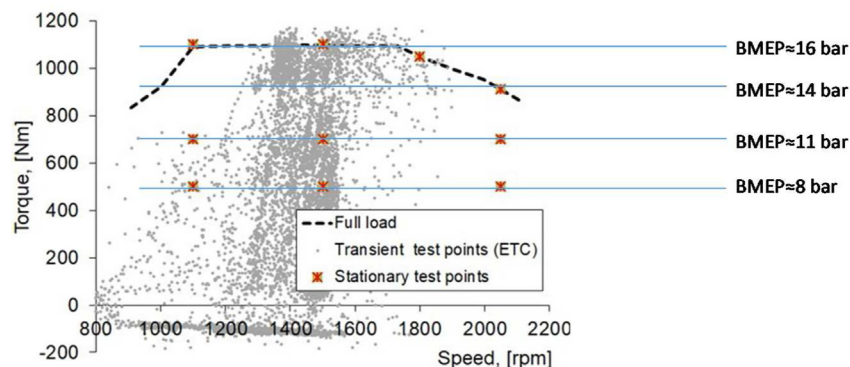
Table 5 – Stationary test points.

Speed (rpm)	Torque (Nm)	BMEP (bar)	Intake manifold air temperature (°C)	Intake manifold air absolute pressure (bar)	Coolant temperature (°C)	Oil pressure (bar)
1100	500	8	35 ± 5	0.9	80 ± 10	4.5 ± 0.3
	700	11	38 ± 5	1.2	80 ± 10	4.5 ± 0.3
	1100	16	41 ± 5	1.8	80 ± 10	4.5 ± 0.3
1500	500	8	35 ± 5	0.9	80 ± 10	4.9 ± 0.3
	700	11	38 ± 5	1.2	80 ± 10	4.9 ± 0.3
	1100	16	41 ± 5	1.8	80 ± 10	4.9 ± 0.3
1800	1050	16	41 ± 5	1.8	80 ± 10	5.0 ± 0.3
2050	500	8	35 ± 5	0.9	80 ± 10	5.2 ± 0.3
	700	11	38 ± 5	1.2	80 ± 10	5.2 ± 0.3
	910	14	40 ± 5	1.6	80 ± 10	5.2 ± 0.3

Tests were performed using CNG with the typical composition of the network gas and two blends with 15% and 25% by volume of hydrogen in CNG. In Table 4 the main characteristics of the tested fuels are reported.

As previously stated, the experimental campaign foresaw tests in stationary and transient conditions. Stoichiometric air to fuel ratio was achieved in closed-loop control also for

hydrogen blend tests. Boosting was managed according to CNG calibrations for all the tested blends. Values of speed, torque, brake mean effective pressure (BMEP), intake air temperature and pressure downstream the throttle valve, coolant temperature and oil pressure of the selected operating points are reported in Table 5.

**Fig. 2 – Operating points during stationary tests and ETC.**

The operating points were selected to cover different areas of the engine working map, at low/medium/high speed and various load conditions, marked with red crosses in Fig. 2. More in detail, as listed in Table 5, ten different engine points were chosen with rotation speeds of 1100 rpm, 1500 rpm, 1800 rpm and 2050 rpm (maximum power rotation speed), comprising four conditions at full load (wide open throttle, WOT, accordingly to maximum load output target programmed in ECU calibration). The operating points have been grouped according to the values of BMEP, reported in Fig. 2, which can be assumed to be almost the same and in any case within the test-to-test repeatability.

The test acquisition lasted 5 min after the engine stabilization and three repetitions were performed in each steady-state condition.

Another part of the activity regarded the evaluation of hydrogen addition in transient conditions, along the ETC, whose operating point area is also evidenced in Fig. 2.

The test methodology for the blends characterization in stationary conditions foresaw two different approaches.

- iso-MFB₅₀ of the pure CNG case to evaluate the effect of the different mixtures at standard CNG combustion phasing calibration;
- iso-NO_x of the pure CNG case to evaluate the influence of hydrogen addition to CNG in terms of engine emissions.

The addition of hydrogen leads to a slight reduction in the fuel flow rate reduction, due to the higher LHV calorific value of H₂ compared to CNG one, but, on the other hand the greater stoichiometric air to fuel ratio of H₂ (reported in Table 4) determines slightly higher air flow values. Under these conditions, absolute and specific NO_x emissions can be considered approximately equivalent. With this premise, the test campaign at iso-NO_x was performed working on absolute (ppm) NO_x, as a matter of operational simplicity, being a direct measurement provided by the exhaust gas analyzer.

Both the conditions were achieved through the regulation of the SA set in the ECU. All other ECU settings have not been modified to evaluate the response of the CNG engine to the hydrogen addition up to 25% by volume, without any component replacements. In this sense, the injection was still controlled by the lambda probe, so determining the injection time, based on the air-fuel ratio to achieve the stoichiometric mixture.

The influence of combustion phasing in terms of engine performance and emissions in both working conditions is described and discussed in the following paragraph.

Results discussion

In the following, the results of the test campaigns in stationary and transient conditions will be illustrated and discussed. The two CNG/H₂ blends results will be compared with the pure CNG case, in terms of combustion and emissions analysis. The transient conditions subsection will also include the analysis of the engine response to the hydrogen addition in terms of

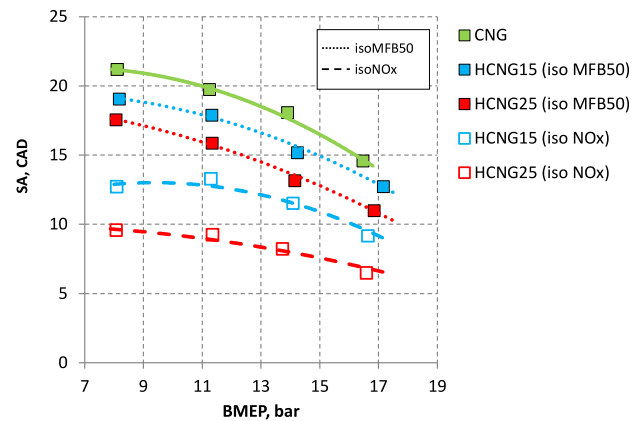


Fig. 3 – SA vs BMEP.

particle number emissions, highlighting its difference with respect to the compressed natural gas fuelling case.

Stationary points

As above introduced, tests in stationary conditions with CNG/H₂ blends were performed acting on SA calibration, to work in iso-MBF₅₀ and iso-NO_x conditions.

Notwithstanding the engine speed affects the combustion evolution (as for example in terms of in-cylinder turbulence), from a preliminary analysis of the results, the authors observed a more marked effect of engine load on emissions. So, in the following graphs and discussion, for an immediate trend analysis, the testing conditions have been grouped over different engine speeds and the results have been averaged over speed and only shown against the BMEP values.

Fig. 3 shows the SA setting versus BMEP in correspondence of the different test cases (iso-MFB₅₀ and iso-NO_x) for all the fuels. In order to easily highlight any significant trends in the two test conditions, in this and next graphs, regression curves of the results are also reported.

SA reduction was always necessary to reach the desired working conditions. During HCNG15 tests, the iso-MFB₅₀ conditions have required a small reduction of SA, about 2 crank angle degree (CAD), with respect to pure CNG fuelling; for the iso-NO_x a further significant reduction, about 4–5 CAD, was necessary, as evidenced in the figure.

The reduction of SA to reach iso-MFB₅₀ and iso-NO_x conditions is ascribable to the high flame speed when burning hydrogen (an order of magnitude faster than NG), as foreseeable. This results in quicker combustion of hydrogen-air mixture in the engine combustion chamber and shorter combustion duration.

Hydrogen addition, in fact, determines a faster combustion advance, especially in the first phase, when the chemical characteristics of the fuels are predominant with respect to the turbulence phenomena. The combustion barycentre should be reached earlier with respect to the pure CNG case, therefore SA has to be reduced to work at same MFB₅₀.

The faster combustion increases temperature values in the combustion chamber and brings to higher NO_x production, as it will be detailed later; a further SA reduction with respect to

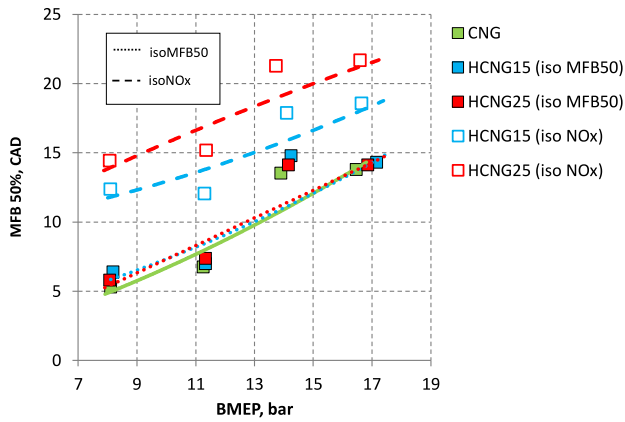


Fig. 4 – MFB₅₀ vs BMEP.

iso-MFB₅₀ case, was necessary to counteract this phenomenon.

When using HCNG25 as fuel, the working conditions were achieved with a greater reduction of the spark advance, as expected at higher hydrogen fraction in the blend. The difference was about 6 CAD for iso-MFB₅₀ case and 8–12 CAD for iso-NO_x case with respect to pure CNG.

The phasing of the combustion barycentre is illustrated in Fig. 4 below. The achievement of almost identical phasing in the iso-MFB₅₀ case for both blends with respect to pure CNG is confirmed in figure. Combustion was delayed in the iso-NO_x case, both for HCNG15 and HCNG25, with HCNG25 presenting a more delayed MFB₅₀, as evidenced.

Graphs in Figs. 5 and 6 highlight combustion characteristics in terms of ignition signal, in-cylinder pressure curve (a) and rate of heat release (ROHR) and heat release percentage (HR%) (b), for the different conditions. For every engine point, the graphs report the average values of three test repetitions. Figs. 5a and 6a, report also the peak firing pressures (PFP) and the maximum values of exhaust temperatures measured in the tested conditions. In particular, Figs. 5 and 6 refer to a test point at medium engine speed (1500 rpm) and load (700 Nm) values (in the next denoted as 1500x700) chosen as example of the iso-MFB₅₀ and iso-NO_x conditions, respectively.

In the iso-MFB₅₀ case, Fig. 5a clearly evidences the shift of the ignition signal increasing the hydrogen percentage. In-cylinder pressure and heat release curves highlight no significant differences among the tested fuels, revealing that the combustion evolution in case of hydrogen addition is generally balanced by SA reduction. As a consequence, almost same peak firing pressures were achieved.

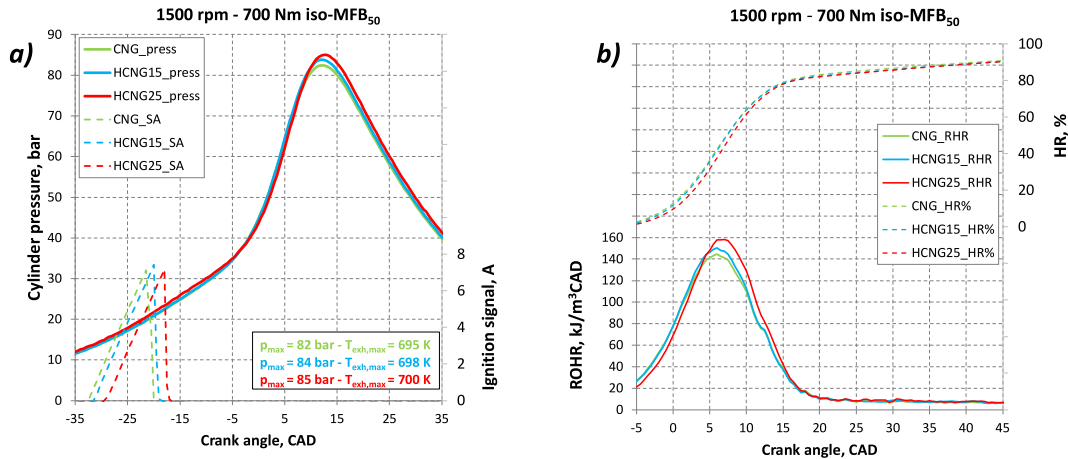


Fig. 5 – Ignition signal and in-cylinder pressure (a), ROHR and HR% (b) at medium speed/load in the iso-MFB₅₀ case.

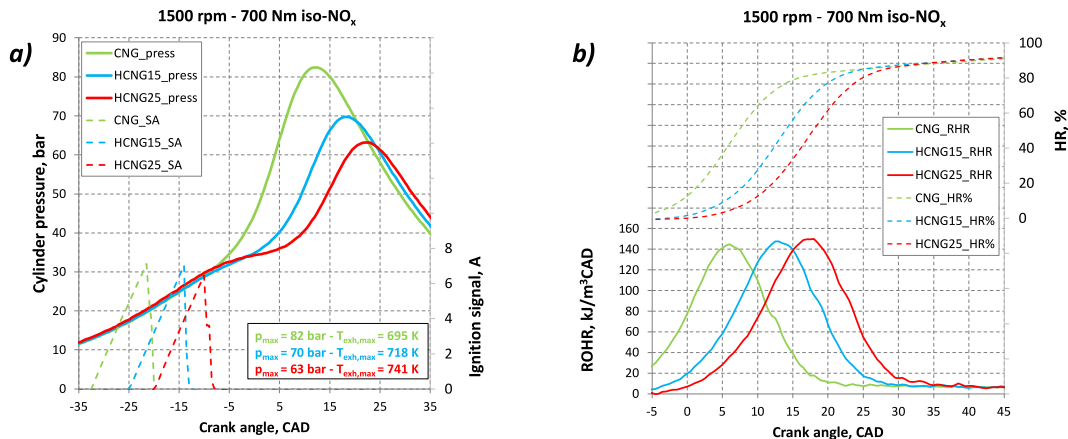


Fig. 6 – Ignition signal and in-cylinder pressure (a), ROHR and HR% (b) at medium speed/load in the iso-NO_x case.

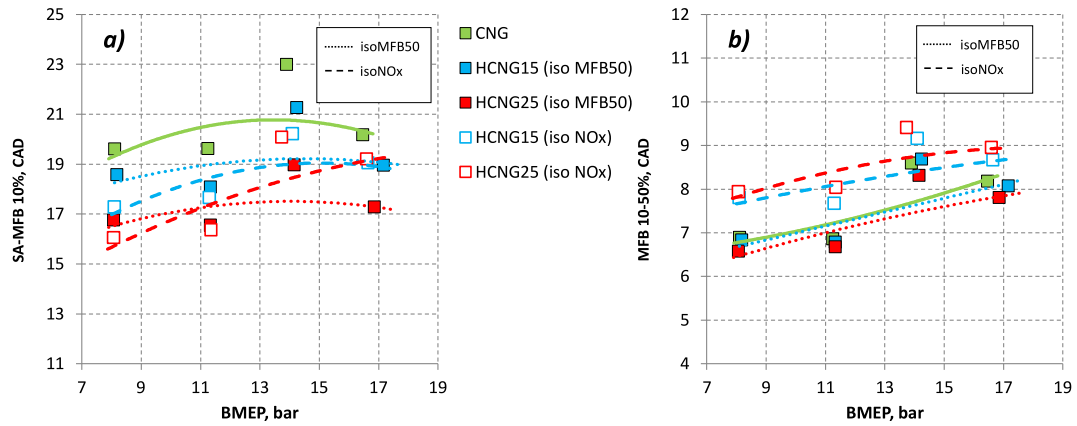


Fig. 7 – Incubation duration (a) and main combustion duration (b).

In the iso-NO_x case (Fig. 6) the differences are more evident; cylinder pressures, ROHR and HR% profiles are delayed with respect to CNG case, in line with the ignition shift. A significant reduction of the PFP is observable (6a), higher as the percentage of hydrogen increases, so bringing to a reduction of efficiency as will be later described.

H₂ addition to the CNG affects the exhaust temperature very slightly and in the iso-MFB₅₀ case no significant differences were found. This confirms that H₂ mainly affects the ID period, no altering the final combustion evolution. Differences in the iso-NO_x cases are greater and mainly due to the different MFB₅₀ phasing through the SA adjustment that brings to a delayed combustion and higher exhaust temperatures. This aspect could be particularly important in relation to the protection of the exhaust components, first of all the turbine.

The combustion analysis helps in the interpretation of the next NO_x emission results.

Fig. 7 shows, for all the fuels and test cases, the duration of two phases of the combustion: ID (7a) e CD (7b).

Incubation duration is shorter for all the considered test conditions, both in case of HCNG15 and HCNG25 with respect to pure CNG. The combustion duration is slightly shorter in the iso-MFB₅₀ cases; a faster initial combustion (near top dead center, TDC) occurred, bringing to the increase in NO_x emissions before introduced.

Iso-NO_x cases have longer CD due to the greater reduction of SA; later combustion phasing was in fact necessary to reduce NO_x emissions at the same level of CNG.

Fig. 8 shows engine-out NO_x emission. As before introduced, a NO_x increment occurred in iso-MFB₅₀ condition, higher for HCNG25. As desired, nitrogen oxides emissions in iso-NO_x case are almost identical to CNG ones, in particular considering HCNG15 mixture, so highlighting that the chosen SA regulation has been sufficient to offset the observed NO_x increment. In the HCNG25 case the interpolation curve amplifies the differences, while the experimental data are more similar to the CNG values. In particular, if it is true that in one point the emissions are higher, in another they are lower than the CNG case, while in the other two (at 8 bar and 16 bar of BMEP) they are very similar to the values of CNG. This is due to slight differences in the engine parameters setting, which sometimes had a spontaneous drift, giving rise to the observed differences. The cylinder pressure evolution with the strong PFP reduction observed in Fig. 6a, clearly justify the benefits on NO_x emissions.

The replacement of CNG with a fraction of H₂ brings to a reduction of unburned hydrocarbon emission for all the cases considered, as it can be seen in Fig. 9. The same for CO emission (not reported here for brevity). This is partially due to the higher H/C ratio of the blends with respect to the pure CNG (see Table 4). Further reduction of emissions could be ascribed

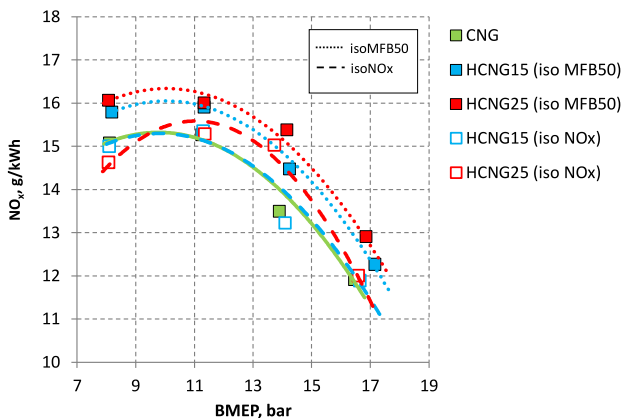


Fig. 8 – NO_x vs BMEP.

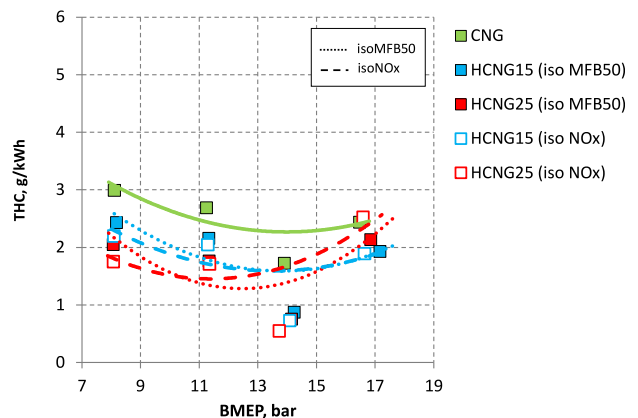


Fig. 9 – THC vs BMEP.

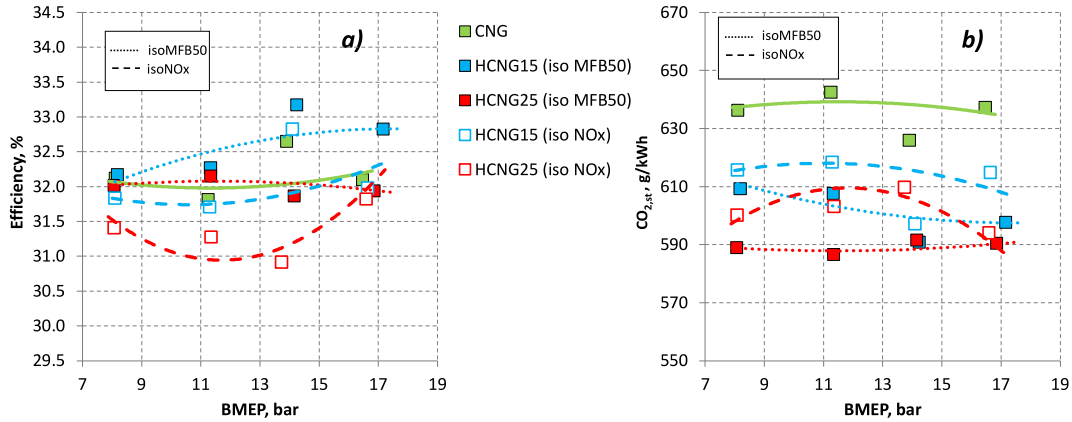


Fig. 10 – Combustion efficiency (a) and CO₂ emissions (b) vs BMEP.

to the slightly higher efficiency of the combustion promoted by H₂, with more hydrocarbon and CO from CNG burning converted into CO₂ during the combustion process. This effect is clearly seen at low and medium loads, with a greater impact in the case of 25% H₂.

The retarded SA timing, corresponding to the iso-NO_x cases, contributes to a further reduction of THC due to the known mechanisms of less fuel trapped in the crevices; this is particularly evident at lower BMEP conditions, where (as confirmed in Fig. 6) the PFP is by far lower burning H₂/CNG mixtures. Differently, at maximum load (17 bar of BMEP) this effect is less marked and the results shown a substantially no variations in unburned emissions level among different H₂ rates or MBF values.

What observed can be confirmed in Fig. 10a that shows the global efficiency (η_g), calculated as:

$$\eta_g = \frac{P_{eff}}{\dot{m}_c * H_i}$$

Where P_{eff} represents the effective power obtained at the

shaft, \dot{m}_c is the burned fuel flow rate and H_i is the lower heating value (LHV). Hydrogen addition slightly improves global efficiency. In fact, efficiency is higher for iso-MFB₅₀ than pure CNG and it is only slightly lower for the iso-NO_x case characterized by a delayed combustion. The presence of hydrogen allows a reduction of CO₂ at the exhaust, that, at equal engine efficiency, can be correlated to the percentage of replacement, apart some iso-NO_x conditions at lower engine efficiency. In fact, the higher combustion speed, occurring when hydrogen blends are burned, required the SA reductions (observed in Fig. 3) to work at the same NO_x levels of pure CNG case. The greater SA reduction of the iso-NO_x with respect to iso-MFB₅₀ conditions, determined, in some cases, more pronounced combustion shift and the resulting reduced efficiency.

European Transient Cycle

The engine response to hydrogen addition was also evaluated in transient condition along European Transient Cycles. ETC is

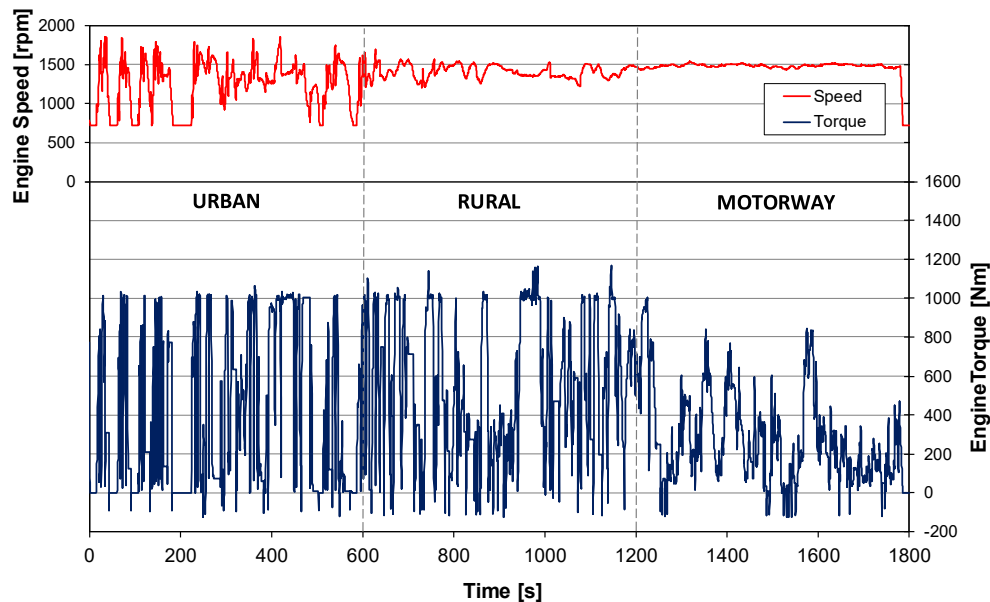


Fig. 11 – ETC engine speed and torque traces.

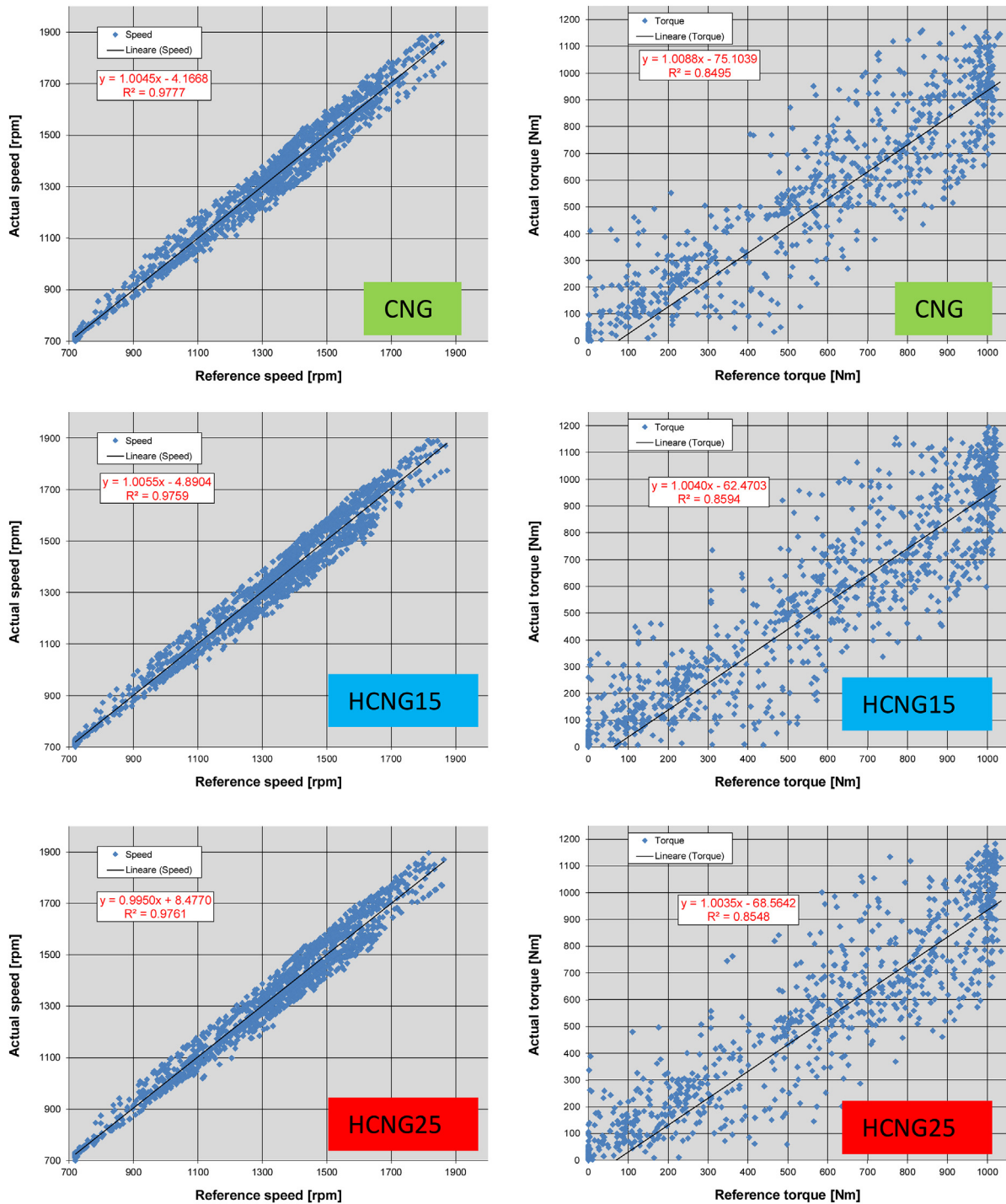


Fig. 12 – Correlation coefficient and linear regression of actual and reference ETC speed and torque data, for CNG and HCNG blends.

the reference cycle for HD gas engine emission measurement in the steps EURO III (where the tested engine belongs), IV, V and enhanced environmental-friendly vehicles (EEV).

The engine speed and torque traces of the ETC are reported in Fig. 11. As shown in the same graph, the cycle comprises three different driving conditions: Urban, representing city driving with frequent starts, stops and idling, Rural, starting

with a steep acceleration segment and Motorway driving. The duration of each part is 600s, for an entire cycle of 1800s.

The testing methodology foresaw to adopt the CNG calibration also in case of hydrogen blends fuelling (no SA variation), in order to evaluate the engine behaviour up to 25% of hydrogen substitution. Two ETC repetitions were performed for each tested fuel.

Table 6 – ETC emission and performance data, for CNG and HCNG blends.

Measured quantities	Unit	CNG	HCNG15	HCNG25
CO	g/kWh	22.7	21.1	20.2
CH ₄	g/kWh	5.2	5.0	4.4
NO _x	g/kWh	15.3	16.2	17.0
CO ₂	g/kWh	723	669	648
BSFC	g/kWh	278	267	259
Energy Consumption	MJ/kWh	12.7	12.3	12.2
Maximum delivered torque	Nm	1240	1288	1300
Maximum delivered power	kW	208	212	212

In the following, the presentation and discussion of the results obtained during the transient tests campaign are reported.

The test cycle reproducibility is analysed in the next two figures. More in details, Fig. 12 reports the actual versus reference values of speed and torque during three ETCs, for CNG (first row), HCNG15 (second row) and HCNG25 (third row) fuelling, chosen as example; same considerations are valid for the other performed cycles. The linear regression analysis of data highlights a good quality of the cycle reproduction, independently from the tested fuel. The accuracy of speed control is very high (see R^2 values), while torque control was less accurate (the latter is controlled directly by the electric brake while the former is controlled by the throttle signal modulated by a proportional-integrative controller).

However, all the cycles performed during this test campaign were in accordance with the margins of error set by the ETC regulations [33].

Some emissions and performance results are summarized in Table 6 where data measured during the ETC tests, for CNG and HCNG blends, are reported. More in details, engine-out CO, CH₄, NO_x, CO₂ emissions, brake specific fuel consumption (BSFC), energy consumption (EC), maximum delivered torque and power, as averaged values of the test repetitions,

are listed. No data on unburned H₂ emissions can be provided by the adopted experimental devices.

The results reveal CO and CH₄ emission reductions, moving from the pure CNG to the blends, greater as the percentage of hydrogen increases. This decrease is due to the higher H/C ratio of the blends with respect to the CNG case and to the combustion improvement, as commented for the stationary cases.

As expectable, NO_x emissions are higher for HCNG15 and HCNG25 due to higher combustion temperatures since the same SA is used for all cases, but the increase is limited (about 10% with respect to the CNG case). Notwithstanding the present values refer to measurements upstream a three-way catalyst (TWC), the authors are confident that such increment could not represent an issue in terms of aftertreatment system performances.

Table 6 also highlights a great reduction of CO₂ emission, of about 7% and 10% with respect to pure CNG, for HCNG15 and HCNG25, respectively. This result is in line with the behaviour observed in stationary conditions and is linked to the substitution of CH₄ with hydrogen and to the general higher combustion efficiency in case of hydrogen blends burning. The BSFC is slightly lower with hydrogen addition. To take into account the different LHV values of the three fuels, the EC was calculated, multiplying BSFC by LHV. Looking at EC values in table it is possible to state that the energy demand in case of blends burning was slightly lower, coherently with the overall tendency observed in steady state test campaign in terms of combustion efficiency and indicated efficiency increments. There is an increase of NO_x emissions due to the higher in cylinder temperature as expectable when hydrogen percentage is increased. This result is very promising as no anomalous combustion was detected from in cylinder pressure signals acquired during the transient cycles.

Fig. 13 shows in-cylinder maximum pressure signals acquired for the three tested fuels in correspondence with the ETC torque trace in the interval 220s–270s, chosen as an example. The graph shows the highest peaks for HCNG25 with

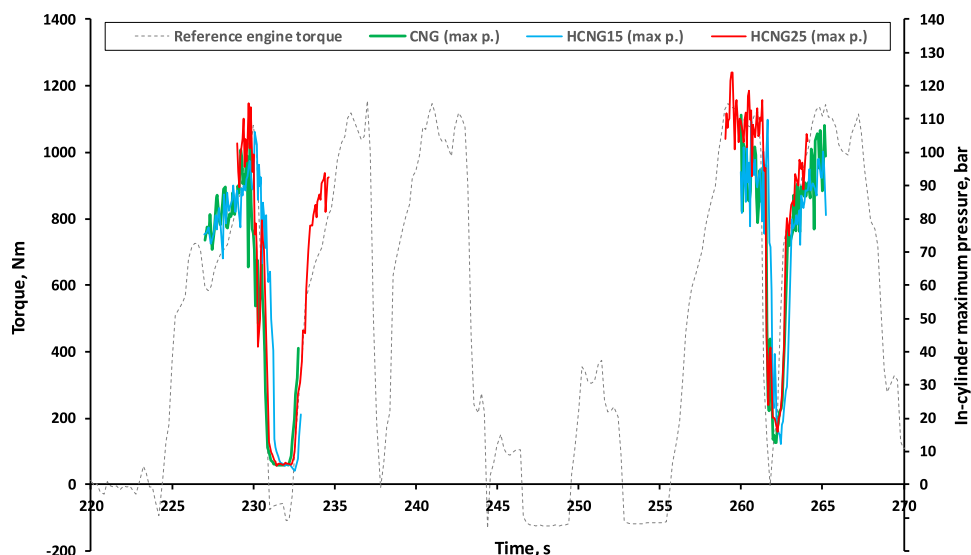


Fig. 13 – Engine torque trace and in-cylinder maximum pressure during an interval of the ETC, for CNG and HCNG blends.

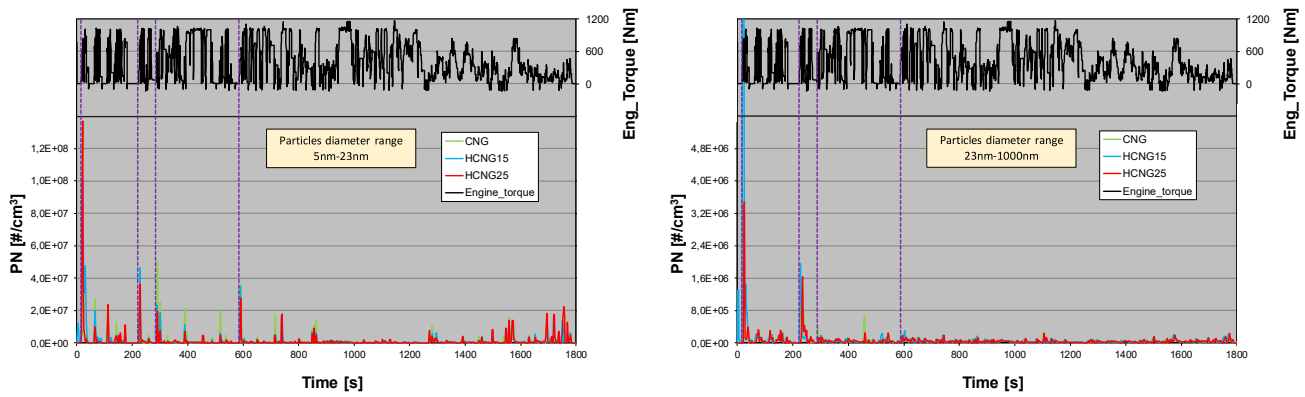


Fig. 14 – Temporal evolution of PN concentration and engine torque traces during ETC; dimensional class 5 nm–23 nm (left), 23 nm–1000nm (right).

delta values of the same amplitude as what was measured in stationary conditions; these increments are anyway in the tolerance range of mechanical stress on cylinder head for the considered class of engine, so should not represent a critical issue. This is an indication that the control of the engine during rapid transients is certainly guaranteed in the case of HCNG25 burning. The ECU, in fact, can manage the closed-loop air index by means of the right gaseous fuel injection time while the SA values set during transients did not compromise the reliability of combustion, so highlighting a good response of the tested engine to a hydrogen addition up to 25% by volume, without any calibration modification.

A part of the activity, still ongoing, regards the analysis of the engine response to hydrogen addition, in terms of engine out particle emissions. The main results of such activity are presented and discussed in the following.

Fig. 14 reports PN emissions temporal evolution (as DMS 500 instrument output) along the entire ETC, for the three tested fuels, together with the engine torque profile. In the present analysis, the total particle population was divided into two dimensional classes: particles with diameters ranging from 23 nm to 1 μm (left side) and particles in the interval between 5 nm and 23 nm (right side), in order to investigate also the emission dynamics of smaller particles belonging to a dimensional range that will be regulated by the next legislation.

The PN profiles clearly highlight the presence of PN emission peaks in correspondence of some phases of the cycle. More in details, the highest peaks occurred during rapid manoeuvres, moving from engine idle to rapid torque increase, highlighted in the graphs by dotted lines. Such behaviour has been already evidenced by the authors during past experiences on a HD gas engine (of similar displacement), methane fuelled, as reported in [34–36]. A possible source of the observed particles emissions is related to the lube oil leakage, favoured by the long idle phases. Many researchers, in fact, agreed on the hypothesis that particle emissions from gas engine are strongly correlated to the lubrication oil leakage between piston and liner [37,38].

Same general PN emission trends were observed for both dimensional classes, with higher PN peaks values in 5 nm–23nm diameters interval.

A consistent fraction of the particles in the 5–23 nm range could be produced by condensation of the oil vapours in the exhaust line, but the present experimental setup did not allow to quantify this aspect, that will be further analysed in next steps of this activity.

Both pure CNG and HCNG blends showed similar PN emission evolution along the transient cycle and analogous correspondence between PN spikes and engine operating condition history.

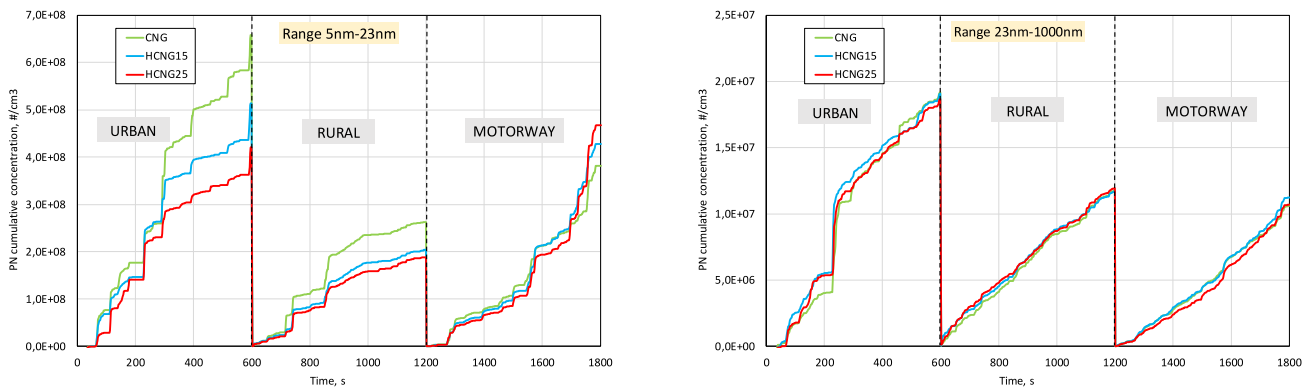


Fig. 15 – Cumulative PN concentration in Urban, Rural and Motorway ETC parts; dimensional class 5 nm–23 nm (left), 23 nm–1000nm (right).

Fig. 15 reports, for CNG and HCNG blends, PN emissions, as cumulative concentration values of particles in the dimensional classes 5 nm–23nm (left side) and 23 nm–1000nm (right side).

As visible from Fig. 14, in the initial phase of the ETC, PN peaks were detected. High variability characterized these peaks, that can be more than an order of magnitude higher than the other spikes recorded during the cycle, so altering the calculated integral value. For this reason, in the cumulative curves the particles emitted in the first 30 s of the cycle were not considered.

The graphs are divided in three parts, separately reporting the results relative to each part of the ETC in order to highlight the contribution of the different phases of the cycle to the cumulative PN and to compare the fuels behaviour in correspondence of the different engine working operations.

As general comment, the graphs confirms that the PN emissions in the 5 nm–23nm range are higher than in the 23 nm–1000nm one. For both the dimensional range, the Urban part, characterized by frequent starts, stops and idling (see Fig. 11) is the most emissive phase of the cycle.

Steps of cumulative emission increase are evident; they are phased, as above observed, with rapid driving condition changes, mainly after engine idle periods and cause the most PN emissions. Such behaviour was common to all the tested fuels, so corroborating the hypothesis that oil leakage events are the cause of such emissions. So, the observed particle formation in hydro methane combustion can be attributed to the incomplete combustion of engine lubricant appearing in small quantities on the cylinder surface.

Looking at sub-23nm particle range, it appears a quite scaled trend of PN, moving from pure CNG case (highest cumulative PN) to HCNG blends, with value decreasing as the percentage of hydrogen increases. Such behaviour is mainly evident in the urban part of the cycle (left side).

This tendency seems to disappear in case of 23 nm–1000nm particles (right side), whereas the three fuels showed similar behaviour.

The trend observed in Fig. 15 suggests a positive effect of hydrogen addition on sub-23 nm particles reduction.

In agreement with literature results [39,40], the measured low particle concentrations can be attributed not only to the presence of a carbon-free fuel leading to the absence of soot agglomerates, but to the superior combustion of the well-premixed hydrogen-air charge.

In fact, as reported in [41], the high diffusion coefficient of hydrogen improves the mixing process. In addition, the high flame speed and smaller quenching distance of hydrogen results in a more complete combustion, which reduces soot formation.

Zhao et al. reported also similar trends reported in Fig. 15, but in case of a DI SI engine using hydrogen and gasoline mixtures. The authors claim that, mainly at low load conditions, blending hydrogen reduces the nucleation mode particles (below 100 nm) more notably than the accumulation mode particles and this might be due to the direct chemically effect of hydrogen blending in inhibiting the growth of polycyclic aromatic hydrocarbons (PAH), that develop into soot particle nuclei when their structures reach a large enough size, as detailed by Guo et al. [42].

Further investigation will be devoted to the analysis of other aspects, as the different behaviour in cold and hot start conditions or the analysis of the chemical/physical features of emitted particles. This information can be useful in view of future aftertreatment systems properly devoted to hydrogen engine emissions control.

Conclusions

The present paper illustrates the main findings of a research activity aimed at analysing the effect of hydrogen addition to a natural gas engine. The discussion is based on experimental data provided by a test campaign on a HD SI engine fuelled with CNG and two different mixtures of CNG and hydrogen (15% and 25% by volume of hydrogen) in steady-state and transient running conditions.

The engine response to hydrogen addition was evaluated in two different conditions.

- at same combustion barycentre of the reference CNG case;
- at same engine out nitrogen oxides emissions of the reference CNG case.

The two conditions were achieved by means of spark advance calibration management. In the first working mode, the faster combustion derived from H₂ addition, led to expectable higher NO_x production, in turn reduced by decreasing the SA set values.

The main findings of such activity can be summarized as follow.

- The presence of H₂ brings to a reduction of unburned hydrocarbon and carbon monoxide emissions.
- Although the faster combustion evolution, the global efficiency is only marginally influenced by the hydrogen content, with a general slight improvement that tends to disappear only for iso-NO_x delayed combustion case. In the same way, a trend of carbon dioxide emission reduction was revealed.
- The combustion analysis, enabled by the adoption of in-cylinder pressure transducer, highlighted the positive result of absence of anomalous combustion in all the tested cases.

The authors intended to evaluate the feasibility of hydrogen addition also in transient condition, running the engine along European transient cycles, but without changing any calibration parameter setting with respect to CNG case.

- Transient tests highlighted a good tolerability of the engine to hydrogen (in the tested percentages) in terms of combustion evolution, as no abnormal combustion phenomena have been detected, even if SA has not been changed.
- A valuable reduction of CO₂ emissions was observed, together with slightly lower energy consumption values.
- Expectable higher engine-out NO_x emissions than that of pure CNG case were revealed, in any case quite limited; future tests will be performed at tailpipe to take into account the TWC efficiency abatement.

The authors are also involved in an experimental activity to characterize particle number emissions when hydro-methane mixtures are used. The present paper reports the main results of such study, aimed at analysing PN engine-out emissions during ETC working conditions.

- Correlation between PN strong emission spikes and rapid engine manoeuvres (from idle to rapid torque/speed variations) have been highlighted for all the tested fuels.
- A trend of PN reduction, mainly in the sub-23nm dimensional range, was revealed by the hydrogen addition.

Further investigation will be necessary to fully characterize particle emissions. In any case, as it stands, the paper already provides useful information on this aspect, expanding the scientific literature, which is rather poor in such data.

The presented results underline that the hydrogen addition up to 25% could be realised in an engine of modern technology without any strong modification and without criticisms in the engine control and management system. This is an interesting output as hydro methane blends can represent, in the next future, a feasible and available alternative fuel in the aim of the urgent decarbonization issue.

Future works will be aimed at verifying the engine response to larger fractions of hydrogen replacing and to pure hydrogen fuelling, also investigating on strategies to counteract the NOx emissions increase, like lean engine operation conditions limits inside acceptable combustion stability.

Declaration of competing interest

The authors declare that they have no known competing financial interests or personal relationships that could have appeared to influence the work reported in this paper.

Acknowledgements

Authors would like to thank Eng. Salvatore Alfuso, Mr Vincenzo Bonanno and Mr. Alessio Schiavone for their technical assistance and support in the engine set-up and testing.

REFERENCES

- [1] Potteau S, Lutz P, Leroux S, Moroz S, Tomas E. Cooled EGR for a turbo SI engine to reduce knocking and fuel consumption (No. 2007-01-3978). SAE Technical Paper; 2007.
- [2] Wei H, Zhu T, Shu G, Tan L, Wang Y. Gasoline engine exhaust gas recirculation—A review. *Appl Energy* 2012;99:534–44.
- [3] Sellnau M, Kunz T, Sinnamon J, Burkhard J. 2-step variable valve actuation: system optimization and integration on an SI engine. *SAE Trans* 2006:13–32.
- [4] Shaik A, Moorthi NSV, Rudramoorthy R. Variable compression ratio engine: a future power plant for automobiles-an overview. *Proc Inst Mech Eng - Part D J Automob Eng* 2007;221(9):1159–68.
- [5] Chaubey R, Sahu S, James OO, Maity S. A review on development of industrial processes and emerging techniques for production of hydrogen from renewable and sustainable sources. *Renew Sustain Energy Rev* 2013;23:443–62.
- [6] Bičáková O, Straka P. Production of hydrogen from renewable resources and its effectiveness. *Int J Hydrogen Energy* 2012;37(16):11563–78.
- [7] Widera B. Renewable hydrogen implementations for combined energy storage, transportation and stationary applications. *Therm Sci Eng Prog* 2020;16:100460.
- [8] Rohendi D, Rahmah DR, Yulianti DH, Amelia I, Sya'baniah NF, Syarif N, Rachmat A. A review on production of hydrogen from renewable sources and applications for fuel cell vehicles. *International Journal of Sustainable Transportation Technology* 2018;1(2):63–8.
- [9] Levene JI, Mann MK, Margolis RM, Milbrandt A. An analysis of hydrogen production from renewable electricity sources. *Sol Energy* 2007;81(6):773–80.
- [10] Eichlseder H, Wallner T, Freymann R, Ringler J. *The potential of hydrogen internal combustion engines in a future mobility scenario* (No. 2003-01-2267. SAE Technical Paper; 2003.
- [11] Braess HH, Strobl W. Hydrogen as a fuel for road transport of the future: possibilities and prerequisites. *HYDROGEN ENERGY PROGRESS* 1996;2:1373–404.
- [12] Teoh YH, How HG, Le TD, Nguyen HT, Loo DL, Rashid T, Sher F. A review on production and implementation of hydrogen as a green fuel in internal combustion engines. *Fuel* 2023;333:126525.
- [13] Bai-gang S, Hua-yu T, Fu-shui L. The distinctive characteristics of combustion duration in hydrogen internal combustion engine. *Int J Hydrogen Energy* 2014;39(26):14472–8.
- [14] Luo QH, Hu JB, Sun BG, Liu FS, Wang X, Li C, Bao LZ. Experimental investigation of combustion characteristics and NOx emission of a turbocharged hydrogen internal combustion engine. *Int J Hydrogen Energy* 2019;44(11):5573–84.
- [15] Sun BG, Zhang DS, Liu FS. Cycle variations in a hydrogen internal combustion engine. *Int J Hydrogen Energy* 2013;38(9):3778–83.
- [16] Shivaprasad KV, Chitragar PR, Nayak V, Kumar GN. Influence of spark timing on the performance and emission characteristics of gasoline–hydrogen-blended high-speed spark-ignition engine. *Int J Ambient Energy* 2017;38(6):605–12.
- [17] Bysveen M. Engine characteristics of emissions and performance using mixtures of natural gas and hydrogen. *Energy* 2007;32(4):482–9.
- [18] Ma F, Wang M, Jiang L, Chen R, Deng J, Naeve N, Zhao S. Performance and emission characteristics of a turbocharged CNG engine fueled by hydrogen-enriched compressed natural gas with high hydrogen ratio. *Int J Hydrogen Energy* 2010;35(12):6438–47.
- [19] Mohammed SE, Baharom MB, Aziz ARA. Analysis of engine characteristics and emissions fueled by in-situ mixing of small amount of hydrogen in CNG. *Int J Hydrogen Energy* 2011;36(6):4029–37.
- [20] Ma F, Wang J, Wang Y, Wang Y, Li Y, Liu H, Ding S. Influence of different volume percent hydrogen/natural gas mixtures on idle performance of a CNG engine. *Energy Fuel* 2008;22(3):1880–7.
- [21] Fu J, Zhong L, Zhao D, Liu Q, Shu J, Zhou F, Liu J. Effects of hydrogen addition on combustion, thermodynamics and emission performance of high compression ratio liquid methane gas engine. *Fuel* 2021;283:119348.
- [22] De Simio L, Gambino M, Iannaccone S. Using Natural Gas/hydrogen mixture as a fuel in a 6-cylinder stoichiometric spark ignition engine. In: *Enriched methane: the first step towards the hydrogen economy*; 2016. p. 175–94.

- [23] Xu H, Ni X, Su X, Xiao B, Luo Y, Zhang F, Yao C. Experimental and numerical investigation on effects of pre-ignition positions on knock intensity of hydrogen fuel. *Int J Hydrogen Energy* 2021;46(52):26631–45.
- [24] Schefer RW, White C, Keller J. Lean hydrogen combustion. In: *Lean combustion*. Academic Press; 2008. 213–VIII.
- [25] Gao W, Fu Z, Li Y, Li Y, Zou J. Progress of performance, emission, and technical measures of hydrogen fuel internal-combustion engines. *Energies* 2022;15(19):7401.
- [26] Lähde T, Giechaskiel B. Particle number emissions of gasoline, compressed natural gas (CNG) and liquefied petroleum gas (LPG) fueled vehicles at different ambient temperatures. *Atmosphere* 2021;12(7):893.
- [27] Thiruvengadam A, Besch MC, Yoon S, Collins J, Kappanna H, Carder DK, Gautam M. Characterization of particulate matter emissions from a current technology natural gas engine. *Environ Sci Technol* 2014;48(14):8235–42.
- [28] Lähde T, Giechaskiel B, Martini G, Howard K, Jones J, Ubhi S. Effect of lubricating oil characteristics on solid particle number and CO₂ emissions of a Euro 6 light-duty compressed natural gas fuelled vehicle. *Fuel* 2022;324:124763.
- [29] Singh AP, Pal A, Agarwal AK. Comparative particulate characteristics of hydrogen, CNG, HCNG, gasoline and diesel fueled engines. *Fuel* 2016;185:491–9.
- [30] Hora TS, Shukla PC, Agarwal AK. Particulate emissions from hydrogen enriched compressed natural gas engine. *Fuel* 2016;166:574–80.
- [31] Thawko A, Tartakovskiy L. The mechanism of particle formation in non-premixed hydrogen combustion in a direct-injection internal combustion engine. *Fuel* 2022;327:125187.
- [32] Symonds JP, Reavell KSJ, Olfert JS, Campbell BW, Swift SJ. Diesel soot mass calculation in real-time with a differential mobility spectrometer. *J Aerosol Sci* 2007;38(1):52–68.
- [33] [https://eur-lex.europa.eu/LexUriServ/LexUriServ.do?uri=OJ:L:2000:044:0001:0155:\[EN:PDF\]](https://eur-lex.europa.eu/LexUriServ/LexUriServ.do?uri=OJ:L:2000:044:0001:0155:[EN:PDF]).
- [34] Napolitano P, Guido C, Beatrice C, Fraioli V, Alfuso S. Particle and gaseous emissions from a heavy-duty SI gas engine over WHTC driving cycles. *SAE International Journal of Advances and Current Practices in Mobility* 2019;2(2019–01-2222):357–67.
- [35] Napolitano P, Alfè M, Guido C, Gargiulo V, Fraioli V, Beatrice C. Particle emissions from a HD SI gas engine fueled with LPG and CNG. *Fuel* 2020;269:117439.
- [36] Guido C, Napolitano P, Alfuso S, Corsetti C, Beatrice C. How engine design improvement impacts on particle emissions from an HD SI natural gas engine. *Energy* 2021;231:120748.
- [37] Thiruvengadam A, Besch MC, Yoon S, Collins J, Kappanna H, Carder DK, Gautam M. Characterization of particulate matter emissions from a current technology natural gas engine. *Environ Sci Technol* 2014;48(14):8235–42.
- [38] Karavalakis G, Hajbabaei M, Jiang Y, Yang J, Johnson KC, Cocker DR, Durbin TD. Regulated, greenhouse gas, and particulate emissions from lean-burn and stoichiometric natural gas heavy-duty vehicles on different fuel compositions. *Fuel* 2016;175:146–56.
- [39] Verhelst S, Wallner T. Hydrogen-fueled internal combustion engines. *Prog Energy Combust Sci* 2009;35(6):490–527.
- [40] Singh AP, Pal A, Agarwal AK. Comparative particulate characteristics of hydrogen, CNG, HCNG, gasoline and diesel fueled engines. *Fuel* 2016;185:491–9.
- [41] Zhao H, Stone R, Zhou L. Analysis of the particulate emissions and combustion performance of a direct injection spark ignition engine using hydrogen and gasoline mixtures. *Int J Hydrogen Energy* 2010;35(10):4676–86.
- [42] Guo H, Liu F, Smallwood GJ, Gülder ÖL. Numerical study on the influence of hydrogen addition on soot formation in a laminar ethylene–air diffusion flame. *Combust Flame* 2006;145(1–2):324–38.